

Search for Invisible Decays of the $\Upsilon(1S)$

B. Aubert,¹ Y. Karyotakis,¹ J. P. Lees,¹ V. Poireau,¹ E. Prencipe,¹ X. Prudent,¹ V. Tisserand,¹ J. Garra Tico,² E. Grauges,² M. Martinelli,^{3a,3b} A. Palano,^{3a,3b} M. Pappagallo,^{3a,3b} G. Eigen,⁴ B. Stugu,⁴ L. Sun,⁴ M. Battaglia,⁵ D. N. Brown,⁵ B. Hooperman,⁵ L. T. Kerth,⁵ Yu. G. Kolomensky,⁵ G. Lynch,⁵ I. L. Osipenkov,⁵ K. Tackmann,⁵ T. Tanabe,⁵ C. M. Hawkes,⁶ N. Soni,⁶ A. T. Watson,⁶ H. Koch,⁷ T. Schroeder,⁷ D. J. Asgeirsson,⁸ C. Hearty,⁸ T. S. Mattison,⁸ J. A. McKenna,⁸ M. Barrett,⁹ A. Khan,⁹ A. Randle-Conde,⁹ V. E. Blinov,¹⁰ A. D. Bukin,^{10,*} A. R. Buzykaev,¹⁰ V. P. Druzhinin,¹⁰ V. B. Golubev,¹⁰ A. P. Onuchin,¹⁰ S. I. Serednyakov,¹⁰ Yu. I. Skovpen,¹⁰ E. P. Solodov,¹⁰ K. Yu. Todyshev,¹⁰ M. Bondioli,¹¹ S. Curry,¹¹ I. Eschrich,¹¹ D. Kirkby,¹¹ A. J. Lankford,¹¹ P. Lund,¹¹ M. Mandelkern,¹¹ E. C. Martin,¹¹ D. P. Stoker,¹¹ H. Atmacan,¹² J. W. Gary,¹² F. Liu,¹² O. Long,¹² G. M. Vitug,¹² Z. Yasin,¹² V. Sharma,¹³ C. Campagnari,¹⁴ T. M. Hong,¹⁴ D. Kovalskyi,¹⁴ M. A. Mazur,¹⁴ J. D. Richman,¹⁴ T. W. Beck,¹⁵ A. M. Eisner,¹⁵ C. A. Heusch,¹⁵ J. Kroseberg,¹⁵ W. S. Lockman,¹⁵ A. J. Martinez,¹⁵ T. Schalk,¹⁵ B. A. Schumm,¹⁵ A. Seiden,¹⁵ L. Wang,¹⁵ L. O. Winstrom,¹⁵ C. H. Cheng,¹⁶ D. A. Doll,¹⁶ B. Echenard,¹⁶ F. Fang,¹⁶ D. G. Hitlin,¹⁶ I. Narsky,¹⁶ P. Ongmongkolkul,¹⁶ T. Piatenko,¹⁶ F. C. Porter,¹⁶ R. Andreassen,¹⁷ G. Mancinelli,¹⁷ B. T. Meadows,¹⁷ K. Mishra,¹⁷ M. D. Sokoloff,¹⁷ P. C. Bloom,¹⁸ W. T. Ford,¹⁸ A. Gaz,¹⁸ J. F. Hirschauer,¹⁸ M. Nagel,¹⁸ U. Nauenberg,¹⁸ J. G. Smith,¹⁸ S. R. Wagner,¹⁸ R. Ayad,^{19,†} W. H. Toki,¹⁹ R. J. Wilson,¹⁹ E. Feltresi,²⁰ A. Hauke,²⁰ H. Jasper,²⁰ T. M. Karbach,²⁰ J. Merkel,²⁰ A. Petzold,²⁰ B. Spaan,²⁰ K. Wacker,²⁰ M. J. Kobel,²¹ R. Nogowski,²¹ K. R. Schubert,²¹ R. Schwierz,²¹ D. Bernard,²² E. Latour,²² M. Verderi,²² P. J. Clark,²³ S. Playfer,²³ J. E. Watson,²³ M. Andreotti,^{24a,24b} D. Bettoni,^{24a} C. Bozzi,^{24a} R. Calabrese,^{24a,24b} A. Cecchi,^{24a,24b} G. Cibinetto,^{24a,24b} E. Fioravanti,^{24a,24b} P. Franchini,^{24a,24b} E. Luppi,^{24a,24b} M. Munerato,^{24a,24b} M. Negrini,^{24a,24b} A. Petrella,^{24a,24b} L. Piemontese,^{24a} V. Santoro,^{24a,24b} R. Baldini-Ferroli,²⁵ A. Calcaterra,²⁵ R. de Sangro,²⁵ G. Finocchiaro,²⁵ S. Pacetti,²⁵ P. Patteri,²⁵ I. M. Peruzzi,^{25,‡} M. Piccolo,²⁵ M. Rama,²⁵ A. Zallo,²⁵ R. Contri,^{26a,26b} E. Guido,^{26a} M. Lo Vetere,^{26a,26b} M. R. Monge,^{26a,26b} S. Passaggio,^{26a} C. Patrignani,^{26a,26b} E. Robutti,^{26a} S. Tosi,^{26a,26b} K. S. Chaisanguanthum,²⁷ M. Morii,²⁷ A. Adametz,²⁸ J. Marks,²⁸ S. Schenk,²⁸ U. Uwer,²⁸ F. U. Bernlochner,²⁹ V. Klose,²⁹ H. M. Lacker,²⁹ T. Lueck,²⁹ A. Volk,²⁹ D. J. Bard,³⁰ P. D. Dauncey,³⁰ M. Tibbetts,³⁰ P. K. Behera,³¹ M. J. Charles,³¹ U. Mallik,³¹ J. Cochran,³² H. B. Crawley,³² L. Dong,³² V. Eyges,³² W. T. Meyer,³² S. Prell,³² E. I. Rosenberg,³² A. E. Rubin,³² Y. Y. Gao,³³ A. V. Gritsan,³³ Z. J. Guo,³³ N. Arnaud,³⁴ J. Béquilleux,³⁴ A. D'Orazio,³⁴ M. Davier,³⁴ D. Derkach,³⁴ J. Firmino da Costa,³⁴ G. Grosdidier,³⁴ F. Le Diberder,³⁴ V. Lepeltier,³⁴ A. M. Lutz,³⁴ B. Malaescu,³⁴ S. Pruvot,³⁴ P. Roudeau,³⁴ M. H. Schune,³⁴ J. Serrano,³⁴ V. Sordini,^{34,§} A. Stocchi,³⁴ G. Wormser,³⁴ D. J. Lange,³⁵ D. M. Wright,³⁵ I. Bingham,³⁶ J. P. Burke,³⁶ C. A. Chavez,³⁶ J. R. Fry,³⁶ E. Gabathuler,³⁶ R. Gamet,³⁶ D. E. Hutchcroft,³⁶ D. J. Payne,³⁶ C. Touramanis,³⁶ A. J. Bevan,³⁷ C. K. Clarke,³⁷ F. Di Lodovico,³⁷ R. Sacco,³⁷ M. Sigamani,³⁷ G. Cowan,³⁸ S. Paramesvaran,³⁸ A. C. Wren,³⁸ D. N. Brown,³⁹ C. L. Davis,³⁹ A. G. Denig,⁴⁰ M. Fritsch,⁴⁰ W. Gradl,⁴⁰ A. Hafner,⁴⁰ K. E. Alwyn,⁴¹ D. Bailey,⁴¹ R. J. Barlow,⁴¹ G. Jackson,⁴¹ G. D. Lafferty,⁴¹ T. J. West,⁴¹ J. I. Yi,⁴¹ J. Anderson,⁴² C. Chen,⁴² A. Jawahery,⁴² D. A. Roberts,⁴² G. Simi,⁴² J. M. Tuggle,⁴² C. Dallapiccola,⁴³ E. Salvati,⁴³ R. Cowan,⁴⁴ D. Dujmic,⁴⁴ P. H. Fisher,⁴⁴ S. W. Henderson,⁴⁴ G. Sciolla,⁴⁴ M. Spitznagel,⁴⁴ R. K. Yamamoto,⁴⁴ M. Zhao,⁴⁴ P. M. Patel,⁴⁵ S. H. Robertson,⁴⁵ M. Schram,⁴⁵ P. Biassoni,^{46a,46b} A. Lazzaro,^{46a,46b} V. Lombardo,^{46a} F. Palombo,^{46a,46b} S. Stracka,^{46a,46b} L. Cremaldi,⁴⁷ R. Godang,^{47,||} R. Kroeger,⁴⁷ P. Sonnek,⁴⁷ D. J. Summers,⁴⁷ H. W. Zhao,⁴⁷ M. Simard,⁴⁸ P. Taras,⁴⁸ H. Nicholson,⁴⁹ G. De Nardo,^{50a,50b} L. Lista,^{50a} D. Monorchio,^{50a,50b} G. Onorato,^{50a,50b} C. Sciacca,^{50a,50b} G. Raven,⁵¹ H. L. Snoek,⁵¹ C. P. Jessop,⁵² K. J. Knoepfel,⁵² J. M. LoSecco,⁵² W. F. Wang,⁵² L. A. Corwin,⁵³ K. Honscheid,⁵³ H. Kagan,⁵³ R. Kass,⁵³ J. P. Morris,⁵³ A. M. Rahimi,⁵³ S. J. Sekula,⁵³ Q. K. Wong,⁵³ N. L. Blount,⁵⁴ J. Brau,⁵⁴ R. Frey,⁵⁴ O. Igonkina,⁵⁴ J. A. Kolb,⁵⁴ M. Lu,⁵⁴ R. Rahmat,⁵⁴ N. B. Sinev,⁵⁴ D. Strom,⁵⁴ J. Strube,⁵⁴ E. Torrence,⁵⁴ G. Castelli,^{55a,55b} N. Gagliardi,^{55a,55b} M. Margoni,^{55a,55b} M. Morandin,^{55a} M. Posocco,^{55a} M. Rotondo,^{55a} F. Simonetto,^{55a,55b} R. Stroili,^{55a,55b} C. Voci,^{55a,55b} P. del Amo Sanchez,⁵⁶ E. Ben-Haim,⁵⁶ G. R. Bonneaud,⁵⁶ H. Briand,⁵⁶ J. Chauveau,⁵⁶ O. Hamon,⁵⁶ Ph. Leruste,⁵⁶ G. Marchiori,⁵⁶ J. Ocariz,⁵⁶ A. Perez,⁵⁶ J. Prendki,⁵⁶ S. Sitt,⁵⁶ L. Gladney,⁵⁷ M. Biasini,^{58a,58b} E. Manoni,^{58a,58b} C. Angelini,^{59a,59b} G. Batignani,^{59a,59b} S. Bettarini,^{59a,59b} G. Calderini,^{59a,59b,¶} M. Carpinelli,^{59a,59b,*} A. Cervelli,^{59a,59b} F. Forti,^{59a,59b} M. A. Giorgi,^{59a,59b} A. Lusiani,^{59a,59c} M. Morganti,^{59a,59b} N. Neri,^{59a,59b} E. Paoloni,^{59a,59b} G. Rizzo,^{59a,59b} J. J. Walsh,^{59a} D. Lopes Pegna,⁶⁰ C. Lu,⁶⁰ J. Olsen,⁶⁰ A. J. S. Smith,⁶⁰ A. V. Telnov,⁶⁰ F. Anulli,^{61a} E. Baracchini,^{61a,61b} G. Cavoto,^{61a} R. Faccini,^{61a,61b} F. Ferrarotto,^{61a} F. Ferroni,^{61a,61b} M. Gaspero,^{61a,61b} P. D. Jackson,^{61a} L. Li Gioi,^{61a} M. A. Mazzoni,^{61a} S. Morganti,^{61a} G. Piredda,^{61a} F. Renga,^{61a,61b} C. Voena,^{61a} M. Ebert,⁶² T. Hartmann,⁶² H. Schröder,⁶² R. Waldi,⁶² T. Adye,⁶³ B. Franek,⁶³ E. O. Olaiya,⁶³ F. F. Wilson,⁶³ S. Emery,⁶⁴ L. Esteve,⁶⁴ G. Hamel de Monchenault,⁶⁴ W. Kozanecki,⁶⁴ G. Vasseur,⁶⁴

Ch. Yèche,⁶⁴ M. Zito,⁶⁴ M. T. Allen,⁶⁵ D. Aston,⁶⁵ R. Bartoldus,⁶⁵ J. F. Benitez,⁶⁵ R. Cenci,⁶⁵ J. P. Coleman,⁶⁵ M. R. Convery,⁶⁵ J. C. Dingfelder,⁶⁵ J. Dorfan,⁶⁵ G. P. Dubois-Felsmann,⁶⁵ W. Dunwoodie,⁶⁵ R. C. Field,⁶⁵ M. Franco Sevilla,⁶⁵ B. G. Fulsom,⁶⁵ A. M. Gabareen,⁶⁵ M. T. Graham,⁶⁵ P. Grenier,⁶⁵ C. Hast,⁶⁵ W. R. Innes,⁶⁵ J. Kaminski,⁶⁵ M. H. Kelsey,⁶⁵ H. Kim,⁶⁵ P. Kim,⁶⁵ M. L. Kocian,⁶⁵ D. W. G. S. Leith,⁶⁵ S. Li,⁶⁵ B. Lindquist,⁶⁵ S. Luitz,⁶⁵ V. Luth,⁶⁵ H. L. Lynch,⁶⁵ D. B. MacFarlane,⁶⁵ H. Marsiske,⁶⁵ R. Messner,^{65,*} D. R. Muller,⁶⁵ H. Neal,⁶⁵ S. Nelson,⁶⁵ C. P. O'Grady,⁶⁵ I. Ofte,⁶⁵ M. Perl,⁶⁵ B. N. Ratcliff,⁶⁵ A. Roodman,⁶⁵ A. A. Salnikov,⁶⁵ R. H. Schindler,⁶⁵ J. Schwiening,⁶⁵ A. Snyder,⁶⁵ D. Su,⁶⁵ M. K. Sullivan,⁶⁵ K. Suzuki,⁶⁵ S. K. Swain,⁶⁵ J. M. Thompson,⁶⁵ J. Va'vra,⁶⁵ A. P. Wagner,⁶⁵ M. Weaver,⁶⁵ C. A. West,⁶⁵ W. J. Wisniewski,⁶⁵ M. Wittgen,⁶⁵ D. H. Wright,⁶⁵ H. W. Wulsin,⁶⁵ A. K. Yarritu,⁶⁵ C. C. Young,⁶⁵ V. Ziegler,⁶⁵ X. R. Chen,⁶⁶ H. Liu,⁶⁶ W. Park,⁶⁶ M. V. Purohit,⁶⁶ R. M. White,⁶⁶ J. R. Wilson,⁶⁶ M. Bellis,⁶⁷ P. R. Burchat,⁶⁷ A. J. Edwards,⁶⁷ T. S. Miyashita,⁶⁷ S. Ahmed,⁶⁸ M. S. Alam,⁶⁸ J. A. Ernst,⁶⁸ B. Pan,⁶⁸ M. A. Saeed,⁶⁸ S. B. Zain,⁶⁸ A. Soffer,⁶⁹ S. M. Spanier,⁷⁰ B. J. Wogland,⁷⁰ R. Eckmann,⁷¹ J. L. Ritchie,⁷¹ A. M. Ruland,⁷¹ C. J. Schilling,⁷¹ R. F. Schwitters,⁷¹ B. C. Wray,⁷¹ B. W. Drummond,⁷² J. M. Izen,⁷² X. C. Lou,⁷² F. Bianchi,^{73a,73b} D. Gamba,^{73a,73b} M. Pelliccioni,^{73a,73b} M. Bomben,^{74a,74b} L. Bosisio,^{74a,74b} C. Cartaro,^{74a,74b} G. Della Ricca,^{74a,74b} L. Lanceri,^{74a,74b} L. Vitale,^{74a,74b} V. Azzolini,⁷⁵ N. Lopez-March,⁷⁵ F. Martinez-Vidal,⁷⁵ D. A. Milanes,⁷⁵ A. Oyanguren,⁷⁵ J. Albert,⁷⁶ Sw. Banerjee,⁷⁶ B. Bhuyan,⁷⁶ H. H. F. Choi,⁷⁶ K. Hamano,⁷⁶ G. J. King,⁷⁶ R. Kowalewski,⁷⁶ M. J. Lewczuk,⁷⁶ I. M. Nugent,⁷⁶ J. M. Roney,⁷⁶ R. J. Sobie,⁷⁶ T. J. Gershon,⁷⁷ P. F. Harrison,⁷⁷ J. Ilic,⁷⁷ T. E. Latham,⁷⁷ G. B. Mohanty,⁷⁷ E. M. T. Puccio,⁷⁷ H. R. Band,⁷⁸ X. Chen,⁷⁸ S. Dasu,⁷⁸ K. T. Flood,⁷⁸ Y. Pan,⁷⁸ R. Prepost,⁷⁸ C. O. Vuosalo,⁷⁸ and S. L. Wu⁷⁸

(BABAR Collaboration)

¹Laboratoire d'Annecy-le-Vieux de Physique des Particules (LAPP), Université de Savoie, CNRS/IN2P3, F-74941 Annecy-Le-Vieux, France

²Universitat de Barcelona, Facultat de Física, Departament ECM, E-08028 Barcelona, Spain

^{3a}INFN Sezione di Bari, I-70126 Bari, Italy

^{3b}Dipartimento di Fisica, Università di Bari, I-70126 Bari, Italy

⁴University of Bergen, Institute of Physics, N-5007 Bergen, Norway

⁵Lawrence Berkeley National Laboratory and University of California, Berkeley, California 94720, USA

⁶University of Birmingham, Birmingham, B15 2TT, United Kingdom

⁷Ruhr Universität Bochum, Institut für Experimentalphysik I, D-44780 Bochum, Germany

⁸University of British Columbia, Vancouver, British Columbia, Canada V6T 1Z1

⁹Brunel University, Uxbridge, Middlesex UB8 3PH, United Kingdom

¹⁰Budker Institute of Nuclear Physics, Novosibirsk 630090, Russia

¹¹University of California at Irvine, Irvine, California 92697, USA

¹²University of California at Riverside, Riverside, California 92521, USA

¹³University of California at San Diego, La Jolla, California 92093, USA

¹⁴University of California at Santa Barbara, Santa Barbara, California 93106, USA

¹⁵University of California at Santa Cruz, Institute for Particle Physics, Santa Cruz, California 95064, USA

¹⁶California Institute of Technology, Pasadena, California 91125, USA

¹⁷University of Cincinnati, Cincinnati, Ohio 45221, USA

¹⁸University of Colorado, Boulder, Colorado 80309, USA

¹⁹Colorado State University, Fort Collins, Colorado 80523, USA

²⁰Technische Universität Dortmund, Fakultät Physik, D-44221 Dortmund, Germany

²¹Technische Universität Dresden, Institut für Kern- und Teilchenphysik, D-01062 Dresden, Germany

²²Laboratoire Leprince-Ringuet, CNRS/IN2P3, Ecole Polytechnique, F-91128 Palaiseau, France

²³University of Edinburgh, Edinburgh EH9 3JZ, United Kingdom

^{24a}INFN Sezione di Ferrara, I-44100 Ferrara, Italy

^{24b}Dipartimento di Fisica, Università di Ferrara, I-44100 Ferrara, Italy

²⁵INFN Laboratori Nazionali di Frascati, I-00044 Frascati, Italy

^{26a}INFN Sezione di Genova, I-16146 Genova, Italy

^{26b}Dipartimento di Fisica, Università di Genova, I-16146 Genova, Italy

²⁷Harvard University, Cambridge, Massachusetts 02138, USA

²⁸Universität Heidelberg, Physikalisches Institut, Philosophenweg 12, D-69120 Heidelberg, Germany

²⁹Humboldt-Universität zu Berlin, Institut für Physik, Newtonstrasse 15, D-12489 Berlin, Germany

³⁰Imperial College London, London, SW7 2AZ, United Kingdom

³¹University of Iowa, Iowa City, Iowa 52242, USA

³²Iowa State University, Ames, Iowa 50011-3160, USA

- ³³*Johns Hopkins University, Baltimore, Maryland 21218, USA*
- ³⁴*Laboratoire de l'Accélérateur Linéaire, IN2P3/CNRS et Université Paris-Sud 11, Centre Scientifique d'Orsay, B. P. 34, F-91898 Orsay Cedex, France*
- ³⁵*Lawrence Livermore National Laboratory, Livermore, California 94550, USA*
- ³⁶*University of Liverpool, Liverpool L69 7ZE, United Kingdom*
- ³⁷*Queen Mary, University of London, London, E1 4NS, United Kingdom*
- ³⁸*University of London, Royal Holloway and Bedford New College, Egham, Surrey TW20 0EX, United Kingdom*
- ³⁹*University of Louisville, Louisville, Kentucky 40292, USA*
- ⁴⁰*Johannes Gutenberg-Universität Mainz, Institut für Kernphysik, D-55099 Mainz, Germany*
- ⁴¹*University of Manchester, Manchester M13 9PL, United Kingdom*
- ⁴²*University of Maryland, College Park, Maryland 20742, USA*
- ⁴³*University of Massachusetts, Amherst, Massachusetts 01003, USA*
- ⁴⁴*Massachusetts Institute of Technology, Laboratory for Nuclear Science, Cambridge, Massachusetts 02139, USA*
- ⁴⁵*McGill University, Montréal, Québec, Canada H3A 2T8*
- ^{46a}*INFN Sezione di Milano, I-20133 Milano, Italy*
- ^{46b}*Dipartimento di Fisica, Università di Milano, I-20133 Milano, Italy*
- ⁴⁷*University of Mississippi, University, Mississippi 38677, USA*
- ⁴⁸*Université de Montréal, Physique des Particules, Montréal, Québec, Canada H3C 3J7*
- ⁴⁹*Mount Holyoke College, South Hadley, Massachusetts 01075, USA*
- ^{50a}*INFN Sezione di Napoli, I-80126 Napoli, Italy*
- ^{50b}*Dipartimento di Scienze Fisiche, Università di Napoli Federico II, I-80126 Napoli, Italy*
- ⁵¹*NIKHEF, National Institute for Nuclear Physics and High Energy Physics, NL-1009 DB Amsterdam, The Netherlands*
- ⁵²*University of Notre Dame, Notre Dame, Indiana 46556, USA*
- ⁵³*Ohio State University, Columbus, Ohio 43210, USA*
- ⁵⁴*University of Oregon, Eugene, Oregon 97403, USA*
- ^{55a}*INFN Sezione di Padova, I-35131 Padova, Italy*
- ^{55b}*Dipartimento di Fisica, Università di Padova, I-35131 Padova, Italy*
- ⁵⁶*Laboratoire de Physique Nucléaire et de Hautes Energies, IN2P3/CNRS, Université Pierre et Marie Curie-Paris6, Université Denis Diderot-Paris7, F-75252 Paris, France*
- ⁵⁷*University of Pennsylvania, Philadelphia, Pennsylvania 19104, USA*
- ^{58a}*INFN Sezione di Perugia, I-06100 Perugia, Italy*
- ^{58b}*Dipartimento di Fisica, Università di Perugia, I-06100 Perugia, Italy*
- ^{59a}*INFN Sezione di Pisa, I-56127 Pisa, Italy*
- ^{59b}*Dipartimento di Fisica, Università di Pisa, I-56127 Pisa, Italy*
- ^{59c}*Scuola Normale Superiore di Pisa, I-56127 Pisa, Italy*
- ⁶⁰*Princeton University, Princeton, New Jersey 08544, USA*
- ^{61a}*INFN Sezione di Roma, I-00185 Roma, Italy*
- ^{61b}*Dipartimento di Fisica, Università di Roma La Sapienza, I-00185 Roma, Italy*
- ⁶²*Universität Rostock, D-18051 Rostock, Germany*
- ⁶³*Rutherford Appleton Laboratory, Chilton, Didcot, Oxon, OX11 0QX, United Kingdom*
- ⁶⁴*CEA, Irfu, SPP, Centre de Saclay, F-91191 Gif-sur-Yvette, France*
- ⁶⁵*SLAC National Accelerator Laboratory, Stanford, California 94309 USA*
- ⁶⁶*University of South Carolina, Columbia, South Carolina 29208, USA*
- ⁶⁷*Stanford University, Stanford, California 94305-4060, USA*
- ⁶⁸*State University of New York, Albany, New York 12222, USA*
- ⁶⁹*Tel Aviv University, School of Physics and Astronomy, Tel Aviv, 69978, Israel*
- ⁷⁰*University of Tennessee, Knoxville, Tennessee 37996, USA*
- ⁷¹*University of Texas at Austin, Austin, Texas 78712, USA*
- ⁷²*University of Texas at Dallas, Richardson, Texas 75083, USA*
- ^{73a}*INFN Sezione di Torino, I-10125 Torino, Italy*
- ^{73b}*Dipartimento di Fisica Sperimentale, Università di Torino, I-10125 Torino, Italy*
- ^{74a}*INFN Sezione di Trieste, I-34127 Trieste, Italy*
- ^{74b}*Dipartimento di Fisica, Università di Trieste, I-34127 Trieste, Italy*
- ⁷⁵*IFIC, Universitat de Valencia-CSIC, E-46071 Valencia, Spain*
- ⁷⁶*University of Victoria, Victoria, British Columbia, Canada V8W 3P6*
- ⁷⁷*Department of Physics, University of Warwick, Coventry CV4 7AL, United Kingdom*
- ⁷⁸*University of Wisconsin, Madison, Wisconsin 53706, USA*

(Received 20 August 2009; published 16 December 2009)

We search for invisible decays of the $Y(1S)$ meson using a sample of 91.4×10^6 $Y(3S)$ mesons collected at the BABAR/PEP-II B factory. We select events containing the decay $Y(3S) \rightarrow \pi^+ \pi^- Y(1S)$

and search for evidence of an undetectable $Y(1S)$ decay recoiling against the dipion system. We set an upper limit on the branching fraction $\mathcal{B}(Y(1S) \rightarrow \text{invisible}) < 3.0 \times 10^{-4}$ at the 90% confidence level.

DOI: 10.1103/PhysRevLett.103.251801

PACS numbers: 13.25.Hw, 11.30.Er, 12.15.Hh

The nature of dark matter is one of the most challenging issues facing physics. Observation of standard model (SM) particles coupling to undetectable (invisible) final states might provide information on candidate dark matter constituents. In the SM, invisible decays of the $Y(1S)$ meson proceed by $b\bar{b}$ annihilation into a $\nu\bar{\nu}$ pair, with a branching fraction $\mathcal{B}(Y(1S) \rightarrow \text{invisible}) \approx 1 \times 10^{-5}$ [1], well below the current experimental sensitivity. However, low-mass dark matter candidates could couple weakly to SM particles to enhance the invisible branching fraction to the level of 10^{-4} to 10^{-3} [2].

Searches for this decay of the $Y(1S)$ can be carried out at e^+e^- colliders operating at the $Y(2S)$ or $Y(3S)$ resonance. The presence of the $Y(1S)$ is tagged by detecting the particles emitted in decays of the resonance to $Y(1S)$. Previous searches by the CLEO [3] and Belle [4] Collaborations yielded upper limits of $\mathcal{B}(Y(1S) \rightarrow \text{invisible}) < 3.9 \times 10^{-3}$ and $< 2.5 \times 10^{-3}$ at the 90% confidence level (C.L.), respectively. In this Letter, we present a search for this final state using almost an order of magnitude more $Y(1S)$ mesons.

The data used in this analysis were collected with the BABAR detector at the PEP-II asymmetric-energy e^+e^- collider running at an e^+e^- center-of-mass (c.m.) energy corresponding to the mass of the $Y(3S)$ ($10.3552 \text{ GeV}/c^2$ [5]). The presence of a $Y(1S)$ meson is tagged by reconstructing the $\pi^+\pi^-$ pair (dipion) in the transition $Y(3S) \rightarrow \pi^+\pi^-Y(1S)$. The BABAR detector is described in detail elsewhere [6]. These data were taken using an upgraded muon system, instrumented with both resistive plate chambers [6] and limited streamer tubes between steel absorbers [7]. For these data, the trigger was modified to substantially increase the dipion trigger efficiency for the signal process. The data sample containing these improvements represents 96.5×10^6 $Y(3S)$ mesons.

We model both generic $Y(3S)$ decays and the signal process using a Monte Carlo (MC) simulation based on GEANT4 [8]. The $Y(3S) \rightarrow \pi^+\pi^-Y(1S)$ events are generated according to the matrix elements measured by the CLEO Collaboration [9]. In signal events, the mass recoiling against the dipion (M_{rec}) peaks at the $Y(1S)$ mass ($9.4603 \text{ GeV}/c^2$ [5]). The same is true for background events in which a real $Y(3S) \rightarrow \pi^+\pi^-Y(1S)$ transition occurs but the $Y(1S)$ final-state particles are undetected (“peaking background”). However, the dominant background containing a pair of low-momentum pions does not exhibit this structure (“nonpeaking background”).

The analysis strategy is as follows: first apply selection criteria to suppress background, primarily the nonpeaking component, then fit the resulting M_{rec} spectrum to measure

the peaking component (signal plus peaking background), and lastly subtract the peaking background, which is mostly from two-body decays of the $Y(1S)$. We define three subsamples for both data and MC events. The first of these, the “invisible” subsample, is designed to contain signal events. Events in this subsample have only two charged pions. The “four-track” subsample is composed of events with two pions plus two tracks with high momenta in the c.m. frame, consistent with two-body decay of the $Y(1S)$ where both final-state particles are detected. It is primarily used to correct the peaking background for imprecisely known branching fractions. The “three-track” subsample is composed of events containing two pions and only one high-momentum track, consistent with two-body $Y(1S)$ decay where only one of the final-state particles is detected. It is used to adjust for inaccuracies in the modeling of track acceptance.

We select events in the invisible subsample by requiring that there are exactly two tracks originating from the interaction point (“IP tracks”) with opposite electric charge. An IP track is required to have a point of closest approach to the interaction point within 1.5 cm in the plane transverse to the beams and within 2.5 cm along the z axis. We further require these tracks to each have c.m.-frame momentum $p^* < 0.8 \text{ GeV}/c$, consistent with pions from the dipion transition. The dipion system is required to have an invariant mass satisfying $M_{\pi\pi} \in [0.25, 0.95] \text{ GeV}/c^2$, compatible with kinematic boundaries ($M_{\pi\pi} \in [2M_\pi, (M_{Y(3S)} - M_{Y(1S)})]$) after allowing for resolution effects. The dipion recoil mass is

$$M_{\text{rec}}^2 = s + M_{\pi\pi}^2 - 2\sqrt{s}E_{\pi\pi}^*, \quad (1)$$

where $E_{\pi\pi}^*$ is the c.m. energy of the dipion system and $\sqrt{s} = 10.3552 \text{ GeV}/c^2$. We require that $M_{\text{rec}} \in [9.41, 9.52] \text{ GeV}/c^2$. The efficiency of this selection for signal events is about 64%, due to the requirement of reconstructing the two pions. All selection criteria were finalized without looking at data in a narrower M_{rec} “signal region” that, according to simulation, contains more than 99% of the signal (see discussion of signal shape below for the precise signal-region definition).

We select three-track and four-track events using the same dipion selection as in the invisible subsample. We search for high-momentum tracks from the $Y(1S)$ decay [i.e., from $Y(1S) \rightarrow e^+e^-$ or $Y(1S) \rightarrow \mu^+\mu^-$]. We require that there be one or two additional IP tracks, each with $p^* > 2.0 \text{ GeV}/c$. If either of these tracks passes electron-identification criteria, both are treated as electrons; otherwise, both are treated as muons. In the former case, we account for possible radiative energy loss due to

bremsstrahlung by pairing an electron with a photon emitted close in angle and increasing the electron's energy and momentum by the energy of this photon. When two high-momentum tracks are present, we require that they have opposite charge and a two-track invariant mass $\in [9.00, 9.80]\text{GeV}/c^2$. We remove photon conversions from these events by rejecting the event if either pion satisfies electron-identification criteria. This introduces a negligible efficiency loss: the probability of a pion to be misidentified as an electron is $\approx 0.1\%$. Finally, we require that the mass difference between the $\pi^+\pi^-\ell^+\ell^-$ and $\ell^+\ell^-$ systems $\in [0.89, 0.92]\text{GeV}/c^2$.

At this stage, the background level in the invisible subsample is several orders of magnitude larger than any hypothetical signal. We reject most of this remaining background with a multivariate analysis (MVA), implemented as a random forest of decision trees [10]. The random forest algorithm is trained on signal-MC events and 5.3% of data outside of the signal region in M_{rec} . The contribution of peaking components to these data is negligible. The data and signal-MC events used to train the MVA are excluded from the rest of the analysis, leaving $91.4 \times 10^6 Y(3S)$ events for use in the final result.

We use the following variables, which have been determined to be only weakly correlated with M_{rec} , as inputs to the MVA: (1) the probability that the pions originate from a common vertex, (2) the laboratory polar angle and transverse momentum of the dipion system, (3) the total number of charged tracks, IP tracks or otherwise, reconstructed in the event, (4) booleans that indicate whether either pion has passed electron, kaon, or muon identification criteria, (5) the cosine of the angle (in the c.m. frame) between the highest-energy photon (γ_1) and the normal to the decay plane of the dipion system, (6) the energy in the laboratory frame of the γ_1 , (7) the total neutral energy in the c.m. frame, and (8) the multiplicity of K_L^0 candidates, defined using the shape and magnitude of the shower resulting from interactions in the calorimeter.

The selection on the MVA output is optimized by choosing the threshold that achieves the minimum statistical uncertainty (dominated by background) on $\mathcal{B}(Y(1S) \rightarrow \text{invisible})$ and, in the null signal hypothesis, the lowest upper limit at the 90% C.L. Both were achieved by requiring an MVA output > 0.8 (where the full range is 0 to 1). The efficiency of this criterion for signal-MC events is 37.0%, as compared to 0.8% for data events outside of the signal region. The total efficiency of all trigger and event selection requirements is determined from signal-MC simulation to be 16.4%.

Figure 1 shows the resulting M_{rec} distribution for events in the invisible subsample. We extract the peaking yield by an extended unbinned maximum likelihood fit, with the nonpeaking background described by a first-order polynomial. The signal and peaking background should have the same shape in M_{rec} . We describe this shape by a modified

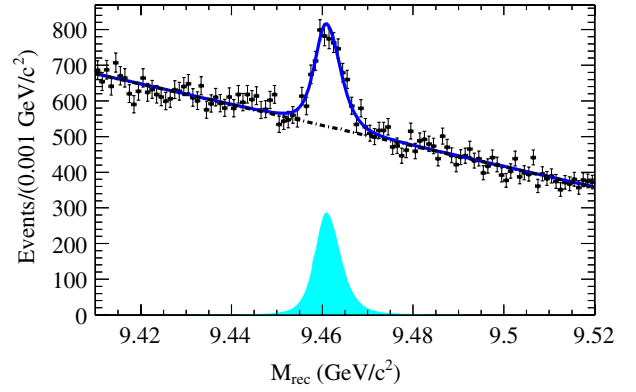


FIG. 1 (color online). The maximum likelihood fit to the dipion recoil mass for data in the invisible subsample. The components of the fit are the nonpeaking background (dash-dotted line) and the peaking component (solid filled line). The total fit function is also shown (solid line). Comparing the fit to the binned data, $\chi^2/(\text{degree of freedom}) = 0.973$.

Gaussian function with a common peak position (μ_0), independent left and right widths ($\sigma_{L,R}$), and non-Gaussian tails (governed by parameters $\alpha_{L,R}$). The functional form on either side of the peak is

$$f_{L,R}(M_{\text{rec}}) = \exp\left[-(M_{\text{rec}} - \mu_0)^2 / (2\sigma_{L,R}^2) + \alpha_{L,R}(M_{\text{rec}} - \mu_0)^2\right]. \quad (2)$$

We determine the parameters of this probability density function (PDF) by fitting M_{rec} in the four-track data subsample. The signal region, excluded when training the MVA, is defined as the region in Fig. 1, which is $< 5\sigma_{L,R}$ from the peak position, $M_{\text{rec}} \in [9.4487, 9.4765] \text{GeV}/c^2$.

The fit to the invisible subsample then determines all of the parameters of the nonpeaking background PDF, the yield of the nonpeaking background, and the yield of the peaking component. Using an MC-based method, we find that the fit accurately returns the peaking contribution over a wide range of input values. The result for the peaking yield in data is 2326 ± 105 events.

Using a second-order polynomial for the nonpeaking background results in no change in the extracted peaking yield. The systematic uncertainty on that yield associated with the fixed parameters in the signal PDF is estimated by varying those parameters in the fit. We find an uncertainty of 18 events.

We next estimate the contribution of background to the peak. The MC simulation predicts 1019 $Y(1S) \rightarrow e^+e^-$ events, 1007 $Y(1S) \rightarrow \mu^+\mu^-$ events, 92 $Y(1S) \rightarrow \tau^+\tau^-$ events, and $2.9 \pm 1.3 Y(1S) \rightarrow \text{hadrons}$ events. These predictions depend upon branching fractions which have significant uncertainties [5] and on the accuracy of the modeling of event reconstruction and selection. We use four-track and three-track data and MC subsamples to test and correct the MC prediction of 2122 total events.

We first use the four-track subsamples to calibrate the product of the branching fractions for $Y(1S) \rightarrow \ell^+ \ell^-$ and $Y(3S) \rightarrow \pi^+ \pi^- Y(1S)$ and the dipion reconstruction efficiency. We compare the event yields between four-track data and MC subsamples when the positively charged lepton is emitted in the central section of the tracking system, $|\cos(\theta_{\ell^+})| < 0.3$ (laboratory-frame angle). The simulation underestimates the number of events in data by a factor of (1.088 ± 0.012) . This is plausible in light of the branching fraction uncertainties [4.7% on the dipion transition, 2.5% on the $Y(1S)$ decay [5]] and track reconstruction uncertainties ($\approx 0.5\%$ per track). Since the effect of the high-momentum track reconstruction has a negligible contribution here, this data or MC correction factor is applied to *all* of our MC-simulation subsamples. For the four-track subsample, Fig. 2(a) shows that the distribution of the high-momentum tracks in the detector is very well described by the MC simulation at all polar angles.

We next compare the data and MC efficiencies for reconstructing the single lepton in the three-track subsample. Any discrepancy would imply a complementary mistake in the invisible peaking background. Given the c.m.-frame polar angle coverage of the detector, for three-track events the high-momentum lepton in the forward direction often escapes detection and thus the detected lepton is in the backward direction. We compare the MC and data laboratory-frame polar angle distributions for these events in Fig. 2(b). The three-track subsample, in contrast to the four-track subsample, has a significant nonpeaking background in recoil mass. Hence three-track peaking yields versus polar angle are determined by using the M_{rec} fit described above and applying an event-weighting technique [11]. The MC simulation describes the distribution well everywhere except at $\cos(\theta_{\ell}) < -0.84$, where the simulation overestimates the reconstruction rate.

For leptons in this far-backward region, we use the ratio of data to simulation versus lepton $\cos(\theta)$ from Fig. 2(b) as the basis of an accept-reject method applied to the high-momentum track. When this method removes the track, it in effect reassigns a three-track event to the invisible

category. We also weight the reassigned events by the ratio of simulated trigger efficiencies for the three-track and invisible subsamples and assign 100% uncertainty to this difference in trigger efficiency. Applying this additive correction after the scaling correction (from the four-track subsample), the total peaking background estimate increases from 2122 events to (2451 ± 38) events.

We test the prediction of the contribution of nonleptonic $Y(1S)$ decays to the peaking background using an additional control sample. Events in this sample contain only two tracks (the pions) and pass all other criteria for the invisible subsample, except that the MVA requirement is replaced by a requirement that the γ_1 has energy > 0.250 GeV. This selects a set of events which is almost disjoint from the invisible subsample, since the MVA > 0.8 requirement results in a steep falloff in efficiency versus γ_1 energy near 0.250 GeV. We compare this energy distribution in data (using the weighting technique [11]) to that from simulation. As the γ_1 energy approaches 0.250 GeV from above, we find that the MC simulation underestimates the data by no more than a factor of 4. Since the expected contribution of these events to the peaking background is 0.14% of the total, we assign 0.6% (15 events) as an additional systematic uncertainty on the peaking background for a total of ± 41 events.

A number of multiplicative systematic corrections and uncertainties to the peaking background also enter, in a fully correlated manner, when the extracted signal yield is converted to the $Y(1S) \rightarrow$ invisible branching fraction. The first such contribution is the 1.088 ± 0.012 correction factor derived from the four-track subsample. But this does not account for trigger and MVA effects which might differ for the invisible and four-track subsamples. Since events used to train the MVA have already passed the trigger requirements, we first study the effect of trigger selection on data. The *BABAR* trigger consists of a hardware and a software stage. The latter is tested by using a heavily prescaled sample of events which bypassed it. We apply the software-level trigger to these events and find that the ratio of efficiencies in data and MC simulation is

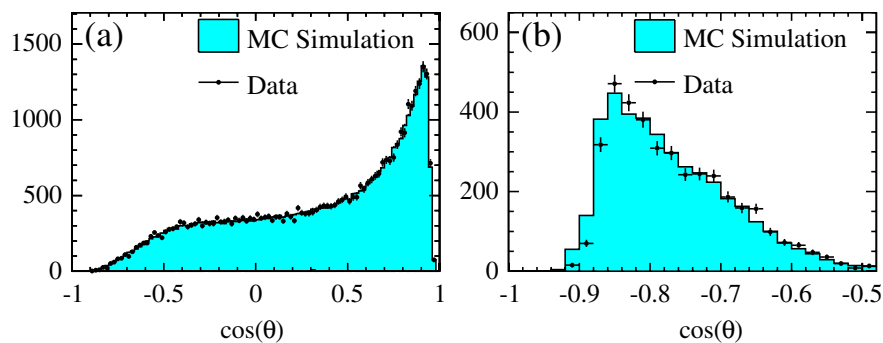


FIG. 2 (color online). The distribution of $\cos(\theta)$, where θ is the laboratory-frame polar angle of (a) the positively charged high-momentum track in the four-track subsample and (b) the single high-momentum track in the three-track subsample. The normalization correction from the four-track subsample has been applied to the MC yields in both cases.

0.997 ± 0.009 . This ratio is taken as a correction to the signal efficiency and the peaking background. To assess how well the impact of the hardware trigger on the two pions is simulated, four-track events are used, since their trigger decision is based largely on the two high-momentum lepton tracks. We apply to the pions a set of selection criteria which approximate those applied by the hardware trigger. The data and MC efficiencies for these requirements differ by 2.2%. Since this test is done on samples for which the hardware trigger is only approximated, we take this difference as a systematic uncertainty rather than apply a correction for it.

After applying the approximate hardware trigger criteria to the four-track subsamples for both $Y(3S)$ MC simulation and data, we apply the nominal MVA selection to both. The relative difference in efficiency between these MC and data subsamples is 4.0%. Since the hardware trigger is again only approximated for this test, we apply no correction for the difference but assign it as a systematic uncertainty on the MVA selection.

Adding the multiplicative uncertainties in quadrature, the total correlated systematic uncertainty is 4.8%. The final corrected prediction for the peaking background is (2444 ± 123) events, including the uncorrelated uncertainty of 41 events. From this we determine the signal yield to be $(-118 \pm 105 \pm 124)$ events, where the errors are statistical and systematic, respectively. To obtain $\mathcal{B}(Y(1S) \rightarrow \text{invisible})$, we divide this by the signal efficiency, the number of $Y(3S)$ mesons, the branching fraction for the dipion transition (4.48% [5]), and the correction factors (1.088×0.997). The factor derived from the four-track subsample includes a possible adjustment of $\mathcal{B}(Y(1S) \rightarrow e^+e^-) + \mathcal{B}(Y(1S) \rightarrow \mu^+\mu^-)$, not relevant for signal. We take this adjustment to be 1.000 ± 0.025 [5] and remove it by assigning an additional systematic uncertainty of 2.5%. Taking correlations into account, we determine that $\mathcal{B}(Y(1S) \rightarrow \text{invisible}) = (-1.6 \pm 1.4(\text{stat}) \pm 1.6(\text{syst})) \times 10^{-4}$.

Lacking evidence for this decay, we use a Bayesian technique to set an upper limit on the branching fraction. We convolute the statistical likelihood, a function of $\mathcal{B}(Y(1S) \rightarrow \text{invisible})$, with Gaussian functions representing the systematic error. We assume a prior probability that is flat in branching fraction and integrate the likelihood from 0 to a value such that 90% of the total integral above 0 is enclosed. The resulting limit is $\mathcal{B}(Y(1S) \rightarrow \text{invisible}) < 3.0 \times 10^{-4}$ at the 90% C.L.

In conclusion, we search for invisible decays of the $Y(1S)$ meson. We do so by looking for evidence of the decay of the $Y(1S)$ into undetectable final states recoiling against the dipion system in $Y(3S) \rightarrow \pi^+\pi^-Y(1S)$, using

a sample of 91.4×10^6 $Y(3S)$ mesons. We find no evidence for $Y(1S) \rightarrow \text{invisible}$ and set an upper limit on its branching fraction at 3.0×10^{-4} at the 90% C.L. This limit is almost an order of magnitude closer to the SM prediction than the best previous limit.

We are grateful for the excellent luminosity and machine conditions provided by our PEP-II colleagues and for the substantial dedicated effort from the computing organizations that support *BABAR*. The collaborating institutions wish to thank SLAC for its support and kind hospitality. This work is supported by DOE and NSF (USA), NSERC (Canada), CEA and CNRS-IN2P3 (France), BMBF and DFG (Germany), INFN (Italy), FOM (The Netherlands), NFR (Norway), MES (Russia), MEC (Spain), and STFC (United Kingdom). Individuals have received support from the Marie Curie EIF (European Union) and the A. P. Sloan Foundation.

*Deceased.

†Now at Temple University, Philadelphia, PA 19122, USA.

‡Also with Università di Perugia, Dipartimento di Fisica, Perugia, Italy.

§Also with Università di Roma La Sapienza, I-00185 Roma, Italy.

||Now at University of South Alabama, Mobile, AL 36688, USA.

¶Also with Laboratoire de Physique Nucléaire et de Hautes Energies, IN2P3/CNRS, Université Pierre et Marie Curie-Paris6, Université Denis Diderot-Paris7, F-75252 Paris, France.

**Also with Università di Sassari, Sassari, Italy.

- [1] L. N. Chang, O. Lebedev, and J. N. Ng, *Phys. Lett. B* **441**, 419 (1998).
- [2] B. McElrath, *Phys. Rev. D* **72**, 103508 (2005).
- [3] P. Rubin *et al.* (CLEO Collaboration), *Phys. Rev. D* **75**, 031104 (2007).
- [4] O. Tajima *et al.* (Belle Collaboration), *Phys. Rev. Lett.* **98**, 132001 (2007).
- [5] C. Amsler *et al.* (Particle Data Group), *Phys. Lett. B* **667**, 1 (2008).
- [6] B. Aubert *et al.* (*BABAR* Collaboration), *Nucl. Instrum. Methods Phys. Res., Sect. A* **479**, 1 (2002).
- [7] W. Menges, *IEEE Nucl. Sci. Symp. Conf. Rec.* **5**, 1470 (2006).
- [8] S. Agostinelli *et al.* (GEANT4 Collaboration), *Nucl. Instrum. Methods Phys. Res., Sect. A* **506**, 250 (2003).
- [9] D. Cronin-Hennessy *et al.*, *Phys. Rev. D* **76**, 072001 (2007).
- [10] L. Breiman, *Mach. Learn.* **45**, 5 (2001).
- [11] M. Pivk and F. R. Le Diberder, *Nucl. Instrum. Methods Phys. Res., Sect. A* **555**, 356 (2005).